THE ASTROPHYSICAL JOURNAL, 232:259–276, 1979 August 15

ACCRETION BY ROTATING MAGNETIC NEUTRON STARS. II. RADIAL AND VERTICAL STRUCTURE OF THE TRANSITION ZONE IN DISK ACCRETION[1]

P. GHOSH
Department of Physics, University of Illinois at Urbana-Champaign
AND
F. K. LAMB[2]
Department of Physics, University of Illinois at Urbana-Champaign; and
California Institute of Technology
Received 1978 August 3; accepted 1979 February 13

ABSTRACT

We investigate the interaction between the stellar magnetic field and the accreting plasma at the magnetospheric boundary of a neutron star accreting matter from a disk. The stellar magnetic field penetrates the inner part of the disk via the Kelvin-Helmholtz instability, turbulent diffusion, and reconnection, producing a broad transition zone joining the unperturbed disk flow far from the star to the magnetospheric flow near the star. Using the two-dimensional hydromagnetic equations, we calculate the inner and outer radii of this zone and its radial and vertical structure. The transition zone is composed of two qualitatively different regions, a broad outer zone where the angular velocity is Keplerian and a narrow inner zone or boundary layer where it departs significantly from the Keplerian value. The star's magnetic field is only slightly deformed within the boundary layer but becomes increasingly distorted at larger radii.

We discuss the implications of the flow solutions found here for neutron-star models of accreting X-ray sources, considering in turn the flow of matter from the inner edge of the disk to the surface of the star, the resulting accretion torque, and the pattern of falling plasma at the stellar surface. Because $\sim 20\%$ of the star's magnetic flux threads the disk outside its inner edge, plasma channeled by the magnetospheric field falls in a circular ring at the magnetic poles.

Subject headings: hydromagnetics — stars: accretion — stars: magnetic — stars: neutron — X-rays: binaries

I. INTRODUCTION

The discovery of more than a dozen pulsating X-ray sources (Pounds 1977; Forman *et al.* 1978) and the strong evidence that these are rotating magnetic neutron stars accreting matter from a binary companion (Lamb 1977; Lightman, Rees, and Shapiro 1978) have generated great interest in the properties of such stars. The changes observed in the pulsation periods of these X-ray sources due to the torque exerted on the star by the accreting matter are particularly significant because they provide the most compelling evidence that the sources are indeed neutron stars (Pringle and Rees 1972; Lamb, Pethick, and Pines 1973; Rappaport and Joss 1977; Mason 1977), and because they furnish clues about the pattern of the accretion flow near the neutron star (Elsner and Lamb 1976; Lamb, Pines, and Shaham 1976, 1978*a*, *b*). Indeed, if our knowledge of accretion flows and the magnetic moments of these stars can be substantially improved, accurate measurements of period changes could provide new constraints on the equation of state of matter at very high densities (Lamb 1977).

In the first paper reporting the results of our study of accretion by rotating magnetic neutron stars (Ghosh, Lamb, and Pethick 1977, hereafter, Paper I), we presented solutions for the flow of accreting matter and the configuration of the magnetic field inside the magnetosphere, and showed that both are strongly influenced by the angular momentum transported to the star by the accreting matter. Pointing out that the torque on the star is determined by matching the flows inside and outside the magnetosphere in a physically acceptable way, we showed that these solutions can be used to derive interesting bounds on the accretion torque even without knowing the details of the flow in the transition zone between the exterior flow and the magnetosphere, by applying general conservation laws. These bounds demonstrate that the early dimensional estimate (Pringle and Rees 1972; Lamb, Pethick, and Pines 1973) of the sign and magnitude of the torque on slowly rotating neutron stars accreting from a disk is correct if the transition zone is narrow, and that in this case this same estimate is also approximately correct even for fast rotators. We considered a variety of exterior flows, and discussed the implications of our

[1] Research supported in part by NSF grant PHY 78-04404 at the University of Illinois and NASA contract NAS5-23315 at Caltech.

[2] Alfred P. Sloan Foundation Research Fellow.

results for secular period changes in pulsating X-ray sources. Finally, we noted that determination of the actual value of the accretion torque does require a detailed description of the flow in the transition zone.

Recently, we have developed a two-dimensional model of steady axisymmetric disk accretion by an aligned rotator which includes a detailed description of the radial and vertical structure of the transition zone and therefore enables us to compute both the innermost radius of the disk and the accretion torque acting on the star. This model represents a first attempt at a consistent description of the flow between the Keplerian region and the stellar surface. We assume that this flow is steady, and use this assumption to determine the effective conductivity of the disk plasma. The resulting dissipation is roughly consistent with that expected from magnetic-flux reconnection. The accretion torque predicted by the model is in good agreement with the observed secular spin-up rates of all the pulsating X-ray sources in which this rate has been measured, including Her X-1, while the short-term period fluctuations and spin-down episodes observed in Her X-1 and Cen X-3 follow naturally from the model as consequences of fluctuations in the mass-accretion rate. In particular, the model predicts a braking torque sufficient to account for the observed spin-down episodes if the accretion rate during the episodes is somewhat reduced. This same braking torque may also explain the paradoxical existence (see Paper I) of a large number of long-period X-ray sources.

In the present paper we provide a detailed account of the accretion flow in this model, including the size and structure of the transition zone and the physical processes that occur there, while in a subsequent paper (Ghosh and Lamb 1979) we calculate the accretion torque predicted by our model, using the flow solutions described here, and compare the implied changes in stellar-rotation rates with those observed. Among the main conclusions reached in the present paper are (1) that the stellar magnetic field threads the disk well beyond its inner edge, and (2) that as a result, the transition zone is not narrow, but instead is rather broad. A brief summary of our principal results has been given previously (Ghosh and Lamb 1978).

In § II we outline the model and the method used to calculate the structure of the accretion flow. We first show that the stellar magnetic field will penetrate the disk over a sizable area as the result of development of the Kelvin-Helmholtz instability, turbulent diffusion, and magnetic-flux reconnection. The stellar field lines that thread the disk are distorted in both the azimuthal and radial directions by the motion of the disk plasma. We assume that in a steady state this distortion of field lines is limited by reconnection, and thereby arrive at the following picture of the accretion flow. Far from the star, the motion of the accreting matter is determined by the effective viscosity in the disk and is unaffected by the stellar magnetic field, but in a broad transition zone between the unperturbed disk and the magnetosphere, the stress associated with the stellar magnetic field becomes increasingly important in determining the flow. The transition zone is composed of two parts, a broad outer part, where the azimuthal velocity is Keplerian, and a narrow inner part where it departs significantly from the Keplerian value.

In § III we set up and solve the hydromagnetic equations in the inner transition zone. This zone behaves like a boundary layer, in that both the flow velocity and the magnetic field change on a length scale $\delta_0 \ll r$. Here screening currents reduce the magnetospheric field typically by a factor of ~ 5, and matter leaves the disk vertically, falling toward the star along stellar field lines.

The structure of the broad outer transition zone is calculated in § IV. Here the magnetic stress carries a significant flux of angular momentum while energy dissipation associated with the motion of the disk plasma across the residual magnetospheric field adds to the heat generated in the disk by viscous dissipation. Even so, the structure of the accretion flow in this zone is very similar to that in a standard α-disk (Shakura and Sunyaev 1973). Currents flowing in this zone screen the residual magnetospheric field to zero on a length scale $\sim r$.

In § V we discuss our flow solutions. First, we argue that the structure of the transition zone found here, namely, a narrow inner zone where most of the screening occurs together with a broad outer zone where the residual stellar flux threads the disk, is likely to be a general feature of disk accretion. Next, we discuss the existence of a maximum stellar-rotation rate consistent with steady accretion, the unusual nature of the inner transition zone, the stability of the flow from the inner edge of the disk to the neutron star, and the implications of our solutions for the pattern of X-ray emission from the stellar surface and period changes in pulsating X-ray sources. We also note some of the new features to be expected in accretion by oblique rotators. Finally, we compare the present calculations with the work of other authors, including the contemporaneous work of Scharlemann (1978) and Ichimaru (1978).

Our main conclusions are summarized in § VI.

II. THE MODEL

In this study we consider disk accretion by a neutron star with a dipolar magnetic field of moment μ. We assume that the star is rotating with angular velocity Ω_s about the magnetic field axis, and that this axis is perpendicular to the plane of the disk. We assume further that the flow is steady and has axial symmetry everywhere. In the mathematical analysis which follows, we use the cylindrical coordinate system (ϖ, ϕ, z) whose origin is at the center of the neutron star and whose polar z-axis lies along the stellar-rotation axis. In this coordinate system, ϕ is the azimuth angle, ϖ is the cylindrical radius, and $r = (\varpi^2 + z^2)^{1/2}$ is the distance from the center of the star. If the disk is thin (semithickness $h \ll r$), then inside it $r \approx \varpi$.

In the present section we first show that complete screening of the stellar magnetic field from the disk plasma is not possible and then introduce a model for

the steady-state configuration of the stellar field lines that thread the disk. Finally, we describe the overall picture of the accretion flow that emerges from our analysis.

a) Failure of Complete Screening in Disk Accretion

The picture of magnetic field screening in the case of roughly spherical accretion by a magnetic neutron star is well known (see Lamb, Pethick, and Pines 1973; Arons and Lea 1976; Elsner and Lamb 1977; Michel 1977*a*, *b*, *c*): currents in the transition region between the magnetosphere and the outside plasma completely screen the stellar magnetic field from the plasma and keep the field confined to the interior of the magnetospheric cavity. This picture is not self-consistent in the case of accretion from a thin disk, however. To see this, suppose that currents on the surfaces of the disk *were* to screen the disk completely. Then the magnetospheric field above and below the disk would be oppositely directed and of magnitude $\sim B_0$, where $B_0 \sim \mu r^{-3}$ is the strength of the unscreened stellar field, and would be completely excluded from the disk. But this configuration will evolve toward one in which the magnetospheric field threads the disk plasma, on a time scale much shorter than the radial drift time of the disk plasma. Thus the original assumption that the magnetospheric field is excluded from the disk is not self-consistent. The field penetrates the disk as a result of a variety of processes, three of which we discuss here:

1. *Kelvin-Helmholtz instability.*—The velocity discontinuity between the low-density magnetic field region and the disk drives the Kelvin-Helmholtz instability with a growth rate[1]

$$\gamma_{\rm KH} \approx (k_\phi^2 v_0^2/c^2 - k_r^2 - k k_g)^{1/2} v_{\rm A}$$

(compare Northrop 1956 and Scharlemann 1978). Here $\boldsymbol{k} = k_r \hat{\boldsymbol{r}} + k_\phi \hat{\boldsymbol{\phi}}$ is the wave vector of the mode, $v_0 = r(\Omega_{\rm K} - \Omega_s) \lesssim 0.1\, c$ is the velocity discontinuity between the disk plasma and the stellar magnetic field in terms of the Keplerian angular velocity $\Omega_{\rm K}$ and the angular velocity Ω_s of the star, $k_g = g_z/v_{\rm A}^2$ is a characteristic wavenumber defined in terms of the magnitude $g_z = (GM/r^2)(h/r)$ of the gravitational acceleration perpendicular to the interface between the magnetic field region and the disk plasma, and $v_{\rm A} = (B_r^2/4\pi\rho)^{1/2}$ is an Alfvén velocity defined in terms of the radial component of the external magnetic field and the plasma density ρ in the disk. This expression for $\gamma_{\rm KH}$ shows that the interface is unstable despite the stabilizing effects of magnetic tension and gravity if $k_\phi > k_r c/v_0 \gg k_r$ and $k(\sim k_\phi)$ is larger than the critical wavenumber $k_c = (c/v_0)^2 k_g$.

For a standard α-disk (Shakura and Sunyaev 1973) and $B_r \sim B_0$, the characteristic wavenumber k_g may be expressed as

$$k_g \approx 1.1 \times 10^{-7} \alpha^{-4/5} \mu_{30}^{-2} (M/M_\odot)^{6/5} \dot{M}_{17}^{3/5} r_8^{12/5}\ {\rm cm}^{-1}, \quad (1)$$

where α is the viscosity parameter of the disk, μ_{30} is μ in units of 10^{30} gauss cm^3, M is the mass of the neutron star, $\dot{M}_{17}$ is the mass-accretion rate $\dot{M}$ in units of 10^{17} g s^{-1}, and r_8 is the radius r in units of 10^8 cm. Thus the critical wavenumber k_c is $\sim 10^2\, k_g \sim 10^3\, r^{-1}$ at $r \sim 10^8$ cm and increases rapidly with increasing radius. Assuming that k_r can be as small as $2\pi/r$, the stabilizing effect of gravity completely dominates that of magnetic tension. Then, for the unstable modes (those with $k > k_c$), the ratio of the radial-drift time in the disk, $\tau_d \sim r|v_r|^{-1}$, to the linear-growth time of the instability $\tau_{\rm KH}$ is

$$\tau_d/\tau_{\rm KH} \sim 1.4 \times 10^5 \alpha^{-5/4} \mu_{30}^{-1} (M/M_\odot)^{5/8} \times (1 - \Omega_s/\Omega_{\rm K})^{-1} r_8^{17/8} (k/k_c)^{1/2}\,. \quad (2)$$

Thus, the Kelvin-Helmholtz instability grows initially on a time scale much shorter than the radial-drift time. Since $k_c h/2\pi \sim 2$ at $r \sim 10^8$ cm, the marginally unstable modes only need to develop a short way into the nonlinear regime for the perturbation δh of the interface to become comparable to h, and we therefore expect the Kelvin-Helmholtz instability to lead to thorough mixing of the disk plasma and the stellar magnetic field in less than the radial-drift time.

2. *Turbulent diffusion.*—If the vertical temperature gradient in the disk leads to vigorous, large-scale convection, as in some disk models (Liang 1977; Shakura, Sunyaev, and Zilitinkevich 1978), and $\rho u_t^2 > B_0^2/8\pi$, where u_t is the rms velocity of the turbulence, the external magnetic field will diffuse vertically through the disk in a time $\tau_t \sim h^2 \eta_t^{-1}$. Here η_t is the turbulent diffusivity, which may be estimated as $0.15\, u_t l_t$ (Parker 1971), where l_t is the length scale of the largest eddies. Using the α-disk relation $u_t l_t \sim \alpha c_s h$, where c_s is the sound velocity, one finds

$$\tau_d/\tau_t \approx 8.6 \times 10^2 \alpha^{1/5} \dot{M}_{17}^{-2/5} (M/M_\odot)^{7/10} r_8^{-1/10}\,. \quad (3)$$

Thus for reasonable values of α ($\gtrsim 10^{-10}$), the external magnetic field will diffuse to the midplane of the disk in less than the radial-drift time.

3. *Reconnection.*—The magnetic field above and below the disk will reconnect to the small-scale magnetic field within the disk plasma, near the top and bottom surfaces of the disk. Subsequent shearing and reconnection of the small-scale magnetic field loops to one another, driven by differential rotation and circulation in convective cells, will cause the magnetospheric field to penetrate inside the disk. The efficiency of this process depends on the strength of the small-scale magnetic field within the disk and the rate of

[1] In the present case, $v_0 \ll c$ and the modes of interest satisfy $k_r \ll k_\phi$. In this regime, the growth rate is almost unaffected by compressibility. One can see this by taking Northrop's expansion scheme to the next higher order; for unstable modes, the growth rate is only increased by an amount

$$\sim \tfrac{1}{4}(v_0/c)^2 (p_{\rm mag}/\rho)(\partial p_{\rm gas}/\partial\rho)^{-1} \lesssim 2 \times 10^{-4} \alpha r_8^{-9/2} (\partial \ln p_{\rm gas}/\partial \ln \rho)^{-1}$$

times the leading term, where $p_{\rm mag}$ is the pressure of the external magnetic field and $p_{\rm gas}$ is the gas pressure in the disk.

reconnection between magnetic fields of unequal strength. If the small-scale magnetic field in the disk is everywhere strong enough to supply most of the effective "viscous" stress (Eardley and Lightman 1975), then it can be shown from the theory of the standard disk that the rms strength of this small-scale field is greater than that of the stellar magnetic field above and below the disk at $r_8 > 1$. Further, if the reconnection rate between magnetic fields of unequal strength is determined by the weaker field, then the relative efficiency of this process is described by the ratio of time scales

$$\tau_d/\tau_R \approx 5 \times 10^3 \xi \alpha^{-7/20} \mu_{30} \dot{M}_{17}{}^{-4/5} (M/M_\odot)^{11/45} r_8{}^{-73/40} . \quad (4)$$

Here we have used the reconnection time scale $\tau_R \approx 2h(\xi v_A)^{-1}$, where v_A is the Alfvén velocity in the weaker reconnecting field and ξ is a numerical factor which depends on the flow pattern (see Vasyliunas 1975). Once again, for reasonable values of ξ the external field will penetrate the disk in a time much shorter than τ_d.

In summary, there are a variety of processes which cause the magnetospheric field to invade and mix with the disk plasma in a time short compared to the radial-drift time. As a result, the stellar magnetic field will thread the disk well beyond its inner edge. Consider now the shape assumed by the magnetic field in a steady state.

b) *Steady-State Configuration*

The angular motion of the disk plasma with respect to the star stretches the stellar field lines in the azimuthal direction, thereby generating a toroidal field B_ϕ from the poloidal field B_p. Similarly, the radial focusing of the flow compresses any azimuthal field that is present, thereby amplifying it. In a steady state, the increase in B_ϕ due to these processes must be exactly balanced by the diffusion of the magnetic field through the disk due to the finite conductivity of the disk plasma. If the effective conductivity of the disk plasma had the usual Coulomb or Bohm value, the equilibrium value of B_ϕ would be extremely large. But long before it becomes this large, the oppositely directed toroidal magnetic fields in the upper and lower halves of the disk reconnect. Thus, the actual value of B_ϕ is determined by a balance between amplification by the plasma flow and reconnection.

Our picture of stellar field lines stretched azimuthally by the different angular velocities of the star and the disk requires the presence of a small amount of plasma on those parts of the field lines which lie between the star and the disk, since if this region were a perfect vacuum, the field lines would continually reconnect there and no toroidal field would develop. However, even a very small quantity of plasma suffices to change the electrodynamic properties of this region from that of a vacuum to that corresponding to our picture. We illustrate this by estimating the number density n of particles above and below the disk required to support the currents implied by the azimuthal pitch given by equation (37) below. Making the reasonable assumption that the plasma in this region is not charge-separated, the required poloidal current $J_p = (c/4\pi)|\nabla \times B_\phi|$ is a conduction current; thus the electron-ion relative velocity can easily be comparable to, but cannot exceed, the local sound speed. If we estimate the sound speed by that in the disk and assume that the azimuthal pitch of a stellar field line threading the disk decreases toward the star on a length scale r, reducing to a very small value at the stellar surface, we obtain

$$n \gtrsim 0.2(\gamma_a/\xi)^2(1 - \Omega_s/\Omega_K) r_8{}^{-2} \text{ cm}^{-3} . \quad (5)$$

Such a small density ($\sim 10^{-21}$ that in the disk) is certain to be present around a neutron star accreting matter from a binary companion. This estimate shows how small a mass in the form of charged particles suffices to change a vacuum electromagnetic field into a typical plasma field, and underscores, as Mestel (1975) has pointed out, the strength of the Coulomb force: although the region above and below the disk is a vacuum, dynamically speaking, it has very non-vacuum electrodynamic properties.

In a manner analogous to the stretching of field lines in the azimuthal direction, the inward radial drift of the disk plasma pinches the stellar field lines inward in the disk plane, thereby generating a radial magnetic field component B_r from the z-component B_z. Again, the radial focusing of the flow amplifies any radial field that is present, and the actual value of B_r is determined by a balance between amplification by the plasma flow and reconnection.

c) *A Self-consistent Picture*

In the next two sections we set up and solve equations which describe in detail the accretion flow and its effect on the stellar magnetic field. It will be helpful, in following this development, to have in mind the overall picture that emerges from our analysis.

The region where the stellar magnetic field threads the disk constitutes a *transition zone* between the unperturbed accretion disk and the magnetosphere. The motion of the disk plasma across the stellar field lines in this transition zone generates currents which confine the stellar magnetic field inside a screening radius r_s, which may be 10–10^2 times larger than the radius r_{co} inside which the plasma is forced to corotate with the star.[2] Thus the transition zone, which extends from

[2] In our brief summary of the present model (Ghosh and Lamb 1978), we followed widespread convention in identifying the corotation radius r_{co}, inside which the plasma is forced to corotate with the star, with the Alfvén radius r_A, inside which the flow is sub-Alfvénic in the stellar magnetic field. Although the definition of the Alfvén radius can be made mathematically precise (see Paper I, § II*b*) and provides a physically meaningful basis for estimating the radius inside which the stellar magnetic field controls the accretion flow (see Lamb, Pethick, and Pines 1973; Elsner and Lamb 1977; Paper I), we do not yet know whether the accretion flow is sub-Alfvénic everywhere between the disk plane and the surface of the star

TABLE 1

DISTINCT REGIONS OF THE ACCRETION FLOW

Region	Inner Radius	Outer Radius	Length Scale of Change in Physical Variables	Dominant Mechanism of Angular Momentum Transport
Unperturbed disk.....	r_s	Large	r	Effective viscous stress
Outer transition zone.....	r_0	r_s	r	Effective viscous stress
Inner transition zone.....	r_{co}	r_0	$\delta_0 \ll r$	Magnetic stress
Magnetosphere.....	R	r_{co}	r	Magnetic stress

r_{co} out to r_s, is quite broad. Within the transition zone the dominant stress transporting the angular momentum of the accreting matter changes from the effective viscous stress to the stress associated with the stellar magnetic field. This zone divides naturally into two parts, an outer part, where the angular velocity is Keplerian, and an inner part, where it departs significantly from the Keplerian value. The boundary between these two parts defines the radius r_0. In § V we argue that this two-part structure of the transition zone is likely to be a general feature of disk accretion.

The *inner transition zone* between r_{co} and r_0 behaves like a boundary layer, in that the flow velocity and the magnetic field change there on a length scale $\delta_0 \ll r_0$. Hence the zone has a thickness $\delta \equiv r_0 - r_{co} \sim \delta_0$ which is small compared to r_0. In this zone the angular velocity of the plasma is reduced from the Keplerian value to the corotational value by the magnetic stress, and circulating currents screen the magnetospheric field, typically by a factor of ~ 5. The inner transition zone or boundary layer is also the region where the dominant magnetic stress disrupts the disk and the accreting matter begins to fall toward the star along the stellar field lines. The set of field lines threading the boundary layer therefore defines the *accretion bundle*, namely, those field lines along which matter accretes onto the star. The plasma in the accretion bundle at the disk plane and just above and below it has significant cross-field motion. Thus the field lines in this region are only approximate streamlines of the flow. As matter falls closer to the star, its cross-field motion is decelerated by the increasing strength of the stellar magnetic field while its field-aligned motion is accelerated by the gravitational force of the star and approaches free fall. There is a *flow-alignment radius* r_f on every field line of the accretion bundle, inside which the cross-field motion of the accreting matter becomes negligible compared with its field-aligned motion. This radius, which must be less than or equal to the Alfvén radius r_A (see Paper I), is in general different on different field lines. Solutions for the field-aligned accretion flow inside r_f have been given in Paper I.

in our model, or even whether this is required for the flow to be stable under the conditions that obtain there (see § V). We have therefore preferred, in the present account, to use a terminology based on the properties of the flow that are calculated here.

The broad *outer transition zone* between r_0 and r_s has a structure very similar to that of a standard disk except for the following modifications caused by the residual stellar magnetic field threading the disk. First, the magnetic stress associated with the twisted stellar field lines transports angular momentum between the disk and the star. Second, the viscous dissipation of energy associated with the effective viscous stress is augmented by the resistive dissipation of energy associated with the cross-field motion of the plasma. Weak screening currents are generated in this zone by the radial cross-field drift of the disk plasma; thus the residual stellar magnetic field which is left after partial screening by the current flowing in the boundary layer is further screened on a length scale $\sim r$ and kept confined within the screening radius r_s which marks the outer edge of the transition zone.

The characteristics of the different regions of the accretion flow are summarized in Table 1.

III. THE BOUNDARY LAYER

In this section we begin our detailed analysis of the flow in the transition zone by calculating the radial and vertical structure of the inner transition zone or boundary layer. We first develop a closed set of equations for the boundary-layer variables and identify the relevant boundary conditions. Next, we show that a boundary layer exists and describe the method used to calculate its structure numerically. Finally, we discuss the characteristics of the boundary layer as a function of the boundary-layer constants and the angular velocity of the star.

a) Equations

The accretion flow and the magnetic field configuration in the boundary layer are described by the following equations.

i) *Radial-Structure Equations*

The radial structure of the boundary layer is described by five basic equations. The first of these is the equation expressing angular-momentum conservation, which may be written in the form

$$d(\dot{M}_d r^2 \Omega)/dr = r^2 \Omega (d\dot{M}_d/dr) + B_\phi B_z r^2 , \quad (6)$$

where $\dot{M}_d(r) = 4\pi r h |v_r| \rho$ is the radial mass-flow rate in the disk plane and Ω is the angular velocity of the

plasma. The two terms on the right-hand side of this equation correspond to the two mechanisms by which angular momentum is transported in the boundary layer; the first describes the angular momentum carried away by the matter leaving the boundary layer vertically while the second represents the angular momentum transported by the magnetic stress. The viscous stress can be neglected, as explained in § V.

The second basic equation, which expresses radial-momentum conservation, is

$$v_r(dv_r/dr) = -GM/r^2 + \Omega^2 r - \rho^{-1}(dp/dr) + (4\pi\rho)^{-1}\{(\nabla \times \boldsymbol{B}) \times \boldsymbol{B}\}\cdot\hat{\boldsymbol{r}} . \quad (7)$$

Here p is the thermal pressure and $\hat{\boldsymbol{r}}$ is a unit vector in the radial direction.

The third and fourth equations are a Maxwell equation,

$$\nabla \times \boldsymbol{B} = 4\pi \boldsymbol{J}/c , \quad (8)$$

and the appropriate version of the generalized Ohm's law, namely,

$$\boldsymbol{J} = \sigma_{\rm eff}(\boldsymbol{E} + c^{-1}\boldsymbol{v} \times \boldsymbol{B}) . \quad (9)$$

Here $\boldsymbol{J}$ is the electric-current density, $\boldsymbol{E}$ is the electric field, and $\sigma_{\rm eff}$ is the effective electrical conductivity of the plasma.

The fifth basic equation is the one which relates the effective conductivity to the flow pattern within the boundary layer. Assuming that the flow is steady, this relationship can be expressed in terms of the average azimuthal pitch,

$$\gamma_\phi = -(B_\phi/B_z)_{z=h} = (B_\phi/B_z)_{z=-h} , \quad (10)$$

at the upper and lower surfaces of the disk. The result, which follows from the radial components of equations (8) and (9), is

$$\sigma_{\rm eff} = (c^2/4\pi)h^{-1}r^{-1}(\Omega - \Omega_s)^{-1}\gamma_\phi . \quad (11)$$

In writing equation (10), we have used the facts that B_ϕ reverses on a length scale h between the upper and lower halves of the disk, and that the radial component of the electric field E_r can be expressed as $E_r = -\Omega_s r B_z c^{-1}$. The latter follows from the observation that when the angular velocity of the plasma exactly equals Ω_s, the magnetic field has no toroidal component and J_r is zero. The value of $\sigma_{\rm eff}$ is a measure of the rate of slippage of field lines through the disk plasma. We emphasize that the value of $\sigma_{\rm eff}$ does not depend on the details of the dissipative process, but only on the assumption of a steady flow: any dissipative process, if it leads to a steady flow, must give an effective conductivity in agreement with equation (11).

ii) *Mass Flow Out of the Disk*

Now consider the vertical mass loss from the boundary layer. We describe this loss by the equation

$$d\dot{M}_d/dr = 4\pi r \rho c_s g(r) , \quad (12)$$

scaling the vertical flow velocity out of the boundary layer in terms of the local sound speed c_s and introducing a "gate" function $g(r)$ which describes the radial profile of mass loss from the boundary layer. Although reconnection of the stellar magnetic field within the boundary layer cannot by itself produce complete threading of the disk plasma by the stellar field, we assume that when it is combined with turbulent diffusion and other dissipative processes, threading is sufficiently complete to channel the flow. We assume further that the flow from the upper and lower surfaces of the disk toward the star is stable. Then the mass-loss profile is largely determined by the shape of the poloidal magnetic field just above and below the boundary layer. Were the dipolar field of the star undistorted, the gravitational potential along each field line would be highest at the magnetic equator, which coincides with the midplane ($z = 0$) of the disk in the present case of an aligned rotator, and matter could flow unimpeded along the magnetic field from the disk toward the star. However, the inward radial motion of the boundary-layer plasma pinches the poloidal field inward, distorting each field line into a shape that has a local minimum of the gravitational potential at the midplane of the boundary layer and two local maxima above and below it (Scharlemann 1978). The mass-loss rate is sensitive to the vertical distance z_m of these maxima from the midplane, since the field lines are approximate streamlines of the flow above and below the disk and hence the accreting matter must flow "over" the maxima of gravitational potential in order to fall toward the star, and since the density of matter varies rapidly with the vertical distance from the midplane [in a standard disk, e.g., ρ drops away from the midplane like $\exp(-z^2/h^2)$].

iii) *Vertical-Structure Equations*

The vertical structure of the boundary layer is determined by three equations: the vertically averaged equations expressing the conservation of vertical momentum and thermal energy, and the equation of state. We write the vertical-momentum equation in the abbreviated form

$$p = C_p \rho (h/r)^2 (GM/r) , \quad (13)$$

where C_p is a number ~ 1, yet to be determined, and we have assumed that the vertical pressure scale height is $\sim h$. The choice $C_p = 1$ would correspond to hydrostatic equilibrium in the vertical direction. In the present case, hydrostatic equilibrium *does not* hold in the vertical direction, since there is vertical mass flow, but the vertical-flow velocity of the matter is $\lesssim c_s$. Hence the vertical-pressure gradient and the vertical component of the gravitational force of the star can differ at most by an amount comparable to each of them, and the existence of vertical mass flow does not invalidate equation (13). On the other hand, equation (13) neglects the vertical gradient of the magnetic pressure. While this is self-consistent near the outer edge of the boundary layer, the solutions obtained below imply that the confining effect of the magnetic

pressure gradient dominates that of gravity in the middle and inner part of the boundary layer, where the density drops sharply because of the increased radial velocity. Thus the present solutions overestimate h and underestimate ρ, T, and p. A fully self-consistent treatment of the vertical structure of the boundary layer must await a detailed calculation of the vertical structure of the magnetic field. The location of the boundary layer and its radial structure are not affected by this approximation.

The equation which describes the vertical radiative transport of the energy generated in the boundary layer, which is dominated by that due to resistive dissipation of the electric current $\boldsymbol{J}$, may be written in the form

$$\tfrac{1}{3}caT^4/\rho h\kappa = (J^2/\sigma_{\rm eff})h\,. \tag{14}$$

Here T is the temperature, a is the radiation constant, and $\kappa = 0.4$ cm^2 g^{-1} is the electron-scattering opacity.

Finally, we adopt an ideal-gas equation of state for the gas-pressure–dominated, fully-ionized plasma,

$$p = \rho(2k_{\rm B}T/m_p)\,, \tag{15}$$

neglecting constituents other than hydrogen. Here $k_{\rm B}$ is Boltzmann's constant and m_p is the proton mass.

b) *Boundary Conditions*

The variables Ω, v_r, B_z, and $\dot{M}_d$ are subject to the following boundary conditions. The angular velocity Ω of the plasma is continuous at $r_{\rm co}$ and r_0, where it takes the values Ω_s and $\Omega_{\rm K}(r_0)$. The radial velocity v_r and the mass flux $\dot{M}_d$ are continuous at r_0, joining smoothly to the corresponding values given by the outer transition-zone solutions at this radius, while B_z takes the value $\mu r_{\rm co}^{-3}$ at $r_{\rm co}$.[3]

The vertical-structure variables ρ, p, T, and h are all continuous at r_0, joining smoothly to their values in the outer transition zone.

c) *Method of Solution*

We solve for the structure of the inner transition zone as follows. First, we show that the hydromagnetic equations exhibit boundary-layer behavior at a characteristic radius, which we denote by r_0. We then eliminate the four vertical-structure variables, ρ, p, T, and h from the radial-structure equations and solve the latter numerically, subject to the boundary conditions given above. Once the radial structure is known, the values of the vertical-structure variables as functions of the radius follow immediately. We turn now to the details.

i) *Existence of a Boundary Layer*

Equations (6)–(15) provide eight equations for the eight variables Ω, v_r, $\boldsymbol{B}$, $\dot{M}_d$, h, T, ρ, and p. From these eight equations we eliminate the four variables that describe the vertical structure of the flow, using equations (12)–(15). We are thus left with four differential equations for the four variables Ω, v_r, $\boldsymbol{B}$, and $\dot{M}_d$ which describe the radial structure of the flow and the vertical mass loss from the disk. That these equations have a boundary-layer–type solution may be seen as follows.

First, let us assume that the Keplerian motion ends at the radius r_0 and that the four radial variables change there on a length scale $\delta_0 \ll r_0$. Then within the boundary layer the natural unit for the radial coordinate is δ_0, so that the independent boundary-layer variable is

$$x \equiv (r - r_{\rm co})/\delta_0\,. \tag{16}$$

The four dependent variables likewise have natural units. We therefore work with dependent boundary-layer variables consisting of the angular velocity scaled in units of the Keplerian angular velocity at r_0,

$$\omega \equiv \Omega/(GMr_0^{-3})^{1/2}\,; \tag{17}$$

the radial velocity scaled in units of the velocity that matter would attain if allowed to fall freely from $r_{\rm co} + \delta_0$ to $r_{\rm co}$ under the action of the gravitational field of the star,

$$u_r \equiv -v_r/[(2GM/r_0)^{1/2}(\delta_0/r_0)^{1/2}]\,; \tag{18}$$

the magnetic field scaled in terms of the unscreened stellar field,

$$b \equiv B_z/B_z(r_{\rm co})\,; \tag{19}$$

and the radial mass-flow rate scaled in terms of the mass-accretion rate,

$$F \equiv \dot{M}_d/\dot{M}\,. \tag{20}$$

Using definitions (16)–(20), the differential equations for Ω, v_r, and $\boldsymbol{B}$ can be rewritten in nondimensional form as

$$d\omega/dx = C_\omega b^2 F^{-1}\,, \tag{21}$$

$$u_r(du_r/dx) = -(1-\omega^2)/2 + C_\omega(\gamma_\phi^2 + 1)u_r^2 b^2 F^{-1}(\omega - \omega_s)^{-1}\,, \tag{22}$$

and

$$db/dx = -C_b b^{3/4} u_r^{9/8} F^{-1/8}(\omega - \omega_s)^{-9/8}\,, \tag{23}$$

where terms of first and higher order in δ_0/r_0 have been neglected. In equations (22) and (23),

$$\omega_s \equiv \Omega_s/(GMr_0^{-3})^{1/2} \approx 0.82(\gamma_\phi^{11/63} C_b^{16/63} C_\omega^{-25/63} C_p^{-8/63}) \times P^{-1}\dot{M}_{17}^{-3/7}\mu_{30}^{6/7}(M/M_\odot)^{-5/7} \tag{24}$$

is the fastness parameter of the rotator (Elsner and Lamb 1977; Paper I), P is the rotation period of the neutron star in seconds, R_6 is the stellar radius in units of 10^6 cm, and L_{37} is the accretion luminosity

[3] Since the screening currents within the boundary layer enhance the magnetic field within the magnetosphere, the true value of B_z at r_0 is somewhat larger than this; however, the correction factor is not large (see § III*d* below).

in units of 10^{37} ergs s^{-1}. Equations (21)–(23) contain the dimensionless parameters

$$C_\omega \equiv 2^{1/2}\gamma_\phi(r_0/r_A^{(0)})^{-7/2}(\delta_0/r_0) \quad (25)$$

and

$$C_b \equiv 6^{1/8}\gamma_\phi^{7/8}C_p^{1/2}(r_0/r_A^{(0)})^{7/16}(\delta_0/r_0)^{25/16}\psi^{-5/4}, \quad (26)$$

which are not determined by the structure equations in the boundary-layer approximation. Here

$$r_A^{(0)} \equiv \mu^{4/7}(2GM)^{-1/7}\dot{M}^{-2/7} \quad (27)$$

is the characteristic Alfvén radius for spherical accretion (Elsner and Lamb 1977) and

$$\psi \equiv [(9\dot{M}^2/32\pi^2)(\bar{\kappa}/ac)(GMr_0)^{1/2}(2k_B/GMm_p)^4]^{1/10}. \quad (28)$$

This expression for ψ can be conveniently evaluated in terms of the height h_s and viscosity parameter α_s of a standard disk transporting no net angular-momentum flux, with the result $\psi = (h_s/r)_0\alpha_s^{1/10} \propto r_0^{1/20}$.

Equations (25) and (26) give the radius r_0 and radial length scale δ_0 within the boundary layer in terms of the dimensionless quantities C_ω, C_b, C_p, γ_ϕ, and ψ. For example, if one neglects the very weak r_0-dependence of ψ and evaluates it at $r_0 = 10^8$ cm with $\alpha_s = 1$, $M = 1\ M_\odot$, and $\dot{M} = 10^{17}$ g s^{-1}, one obtains

$$\delta_0 = 0.031(\gamma_\phi^{-16/27}C_b^{16/27}C_\omega^{2/27}C_p^{-8/27})r_0 \ll r_0 \quad (29)$$

and

$$r_0 \approx 0.41(\gamma_\phi^{11/27}C_b^{16/27}C_\omega^{-25/27}C_p^{-8/27})^{2/7}r_A^{(0)}. \quad (30)$$

Thus, the boundary-layer approximation is self-consistent. Since $\delta_0/r_0 \propto \alpha_s^{2/27}$ and $r_0 \propto \alpha_s^{4/189}$, both are quite insensitive to the effective viscosity in the disk.

ii) *Internal Structure of the Boundary Layer*

Equation (12), which describes the mass loss from the disk plane, can now be recast in nondimensional form using equations (13)–(20) and (29), with the result

$$dF/dx \approx 0.125(\gamma_\phi^{-8/27}C_b^{8/27}C_\omega^{1/27}C_p^{19/54})g(x)Fu_r^{-1}. \quad (31)$$

This equation and equations (21)–(23) form a complete set for the radial-structure variables and can be solved numerically for a rotator of given fastness, if the azimuthal pitch $\gamma_\phi(x)$, the gate function $g(x)$, and the boundary-layer constants C_b, C_ω, and C_p are known. With the resulting knowledge of ω, u_r, b, and F, the variables

$$\epsilon \equiv h/h_s, \quad \theta \equiv T/T_s, \quad \zeta \equiv \rho/\rho_s, \quad \text{and} \quad \chi \equiv p/p_s, \quad (32)$$

which specify the vertical semithickness, temperature, density, and pressure in the boundary layer in terms of the corresponding quantities in a standard disk (denoted by a subscript s) at the same radius, can be calculated from the vertical-structure equations and the equation of state, completing the boundary-layer solution.

For the solutions presented here, we make the following choice for the functions $\gamma_\phi(x)$ and $g(x)$ and the constants C_b, C_ω, and C_p. First, we take $\gamma_\phi(x) =$ const. $= \gamma_0$ in the boundary layer. The structure of the boundary layer is relatively insensitive to the precise value of γ_0, as may be seen from the solutions for several values of γ_0 in the range 0.5–5 which are described below. Second, we note that the gate function $g(x)$ can be determined accurately by an iterative procedure in which the magnetic field configuration for an assumed $g(x)$ is calculated and checked for self-consistency. However, use of this procedure must await a quantitative description of the accretion flow and the magnetic field configuration in the region between r_0 and the flow-alignment radius r_f. Nevertheless, the other properties of the model are insensitive to the precise form of $g(x)$, provided that $g(x)$ satisfies the conditions (1) that $g \approx 0$ at and outside the outer edge of the boundary layer, and (2) that $g = 1$ well inside the boundary layer. These conditions ensure that essentially all the accreting matter leaves the disk plane within the boundary layer. We assume that the gate function satisfies these conditions, and therefore adopt a simple mass-loss profile for the results reported in this paper, namely,

$$g(x) = 1, \qquad 0 \le x \le x_m,$$
$$= (x_0 - x)^2(x_0 - x_m)^{-2}, \quad x_m \le x \le x_0,$$
$$\text{with } x_0 - x_m = 0.6. \quad (33)$$

Here $x_0 = \delta/\delta_0$ in terms of the width δ of the boundary layer and δ_0. With this gate function, the mass-loss rate saturates by the time the point x_m is reached in the boundary layer. Finally, we take values ~ 1 for the boundary-layer constants C_b, C_ω, C_p, and γ_0.[4] The qualitative structure of the boundary layer is quite insensitive to the values of these constants, as shown below.

In fact, only three of the four constants C_b, C_ω, C_p, and γ_0 can be chosen independently, since the fourth is determined by a constraint derived from the condition that the viscous stress be negligible compared with the magnetic stress at r_0. This constraint follows immediately from the α-model for the disk and the assumption that the azimuthal velocity begins to depart from the Keplerian value at r_0 and is, in nondimensional form,

$$C_b^{-8/27}C_\omega^{25/54}C_p^{4/27}\gamma_0^{8/27} = 0.125b_0^{-1}, \quad (34)$$

where $b_0 = b(x_0)$. It can be deduced by combining equation (35), introduced below, and equation (30).

[4] One expects $\gamma_0 \sim 1$ from the picture of magnetic-flux reconnection in the boundary layer (see § V).

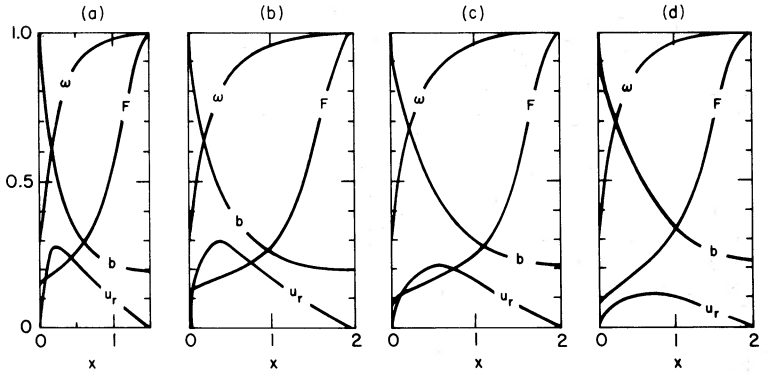

FIG. 1.—Radial structure of the boundary layer for a star of fastness $\omega_s = 0.3$. Shown are the magnetic field b, angular velocity ω, radial velocity u_r, and radial mass-flow rate F, in appropriate dimensionless units (see text) for the following values of the boundary-layer constants: (*a*) $\gamma_0 = 0.5$, $C_b = 2.5$, $C_p = 2$; (*b*) $\gamma_0 = 1$, $C_b = 1.5$, $C_p = 1.5$; (*c*) $\gamma_0 = 2$, $C_b = 2$, $C_p = 1.5$; (*d*) $\gamma_0 = 4$, $C_b = 4$, $C_p = 1$. These cases illustrate the insensitivity of the boundary-layer structure to the values of the boundary-layer constants.

We incorporate constraint (34) into our solutions by adjusting C_ω according to the following iterative method. First, we fix the constants C_b, C_p, and γ_0. Next we choose an initial value for the constant C_ω, solve equations (21)–(23) and (31) to obtain b_0, calculate C_ω from equation (34), and check the initial and final values of C_ω for self-consistency. We then choose a new value of C_ω, iterating until a self-consistent value is obtained.

d) Examples of Boundary-Layer Structure

We now describe the calculated structure of the boundary layer in some typical cases selected from the large number of examples that we have calculated. Each case is labeled by four numbers, namely, the values of the boundary-layer constants, C_b, C_p, and γ_0, and the value of the fastness parameter ω_s.

The structure of the boundary layer is very insensitive to the particular values of the boundary-layer constants, C_b, C_p, and γ_0, a property characteristic of boundary layers generally. This is illustrated in Figure 1, which shows the radial structure for $\omega_s = 0.3$ and various values of the boundary-layer constants. This insensitivity demonstrates that the basic structure of the boundary layer presented here is quite general, and that the actual values of the boundary-layer constants are not crucial to the theory. Henceforth we shall adopt the values $C_b = 2.5$, $C_p = 2$, and $\gamma_0 = 1$.

Figure 2 shows the radial structure of the boundary layer for three different values of ω_s. The currents circulating in the boundary layer screen the magnetospheric field by a factor $b_0 \sim 0.2$. The angular velocity of the matter, which is Keplerian at the outer edge, is reduced by the magnetic stresses in crossing the layer, and reaches corotation at the inner edge. The radial velocity of the matter equals the slow radial drift characteristic of the outer transition zone at r_0, as required by the velocity boundary condition; within the boundary layer it first increases inward as centrifugal support fails and then passes through a maximum and decreases inward as the opposing magnetic pressure gradient becomes very large, finally vanishing at the inner edge of the boundary layer. The maximum value reached by $|v_r|$ in the boundary layer declines systematically as the angular velocity of the star increases, but is typically ~ 0.1–$0.3(2GM/r_0)^{1/2}(\delta_0/r_0)^{1/2}$. The radial mass flux F decreases inward steeply and monotonically in all cases.

Because the screening currents in the boundary layer enhance the stellar magnetic field in the magnetosphere, the value of μ in equation (24) and those that follow should be somewhat larger than the true dipole moment of the star. The factor of enhancement has been found to be in the range 1.7–3 in previous studies of static screening of the magnetospheric field by plasma (Cole and Huth 1959; Midgley and Davis 1962; Arons and Lea 1976; Elsner and Lamb 1977). The enhancement should be smaller in the present

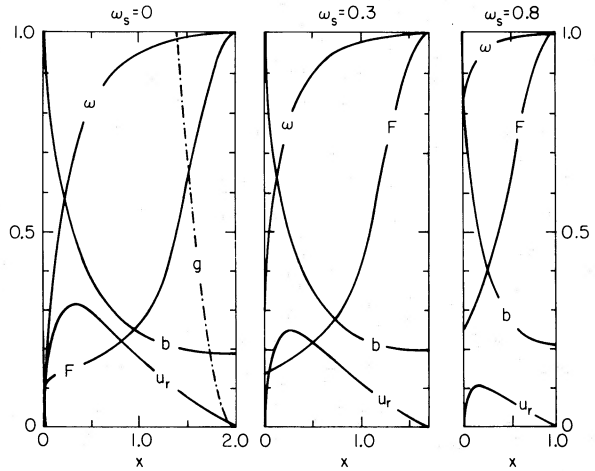

FIG. 2.—Radial structure of the boundary layer for three values of the fastness parameter ω_s, and the canonical values of the boundary-layer constants, namely, $\gamma_0 = 1$, $C_b = 2.5$, and $C_p = 2$. The variables are the same as in Fig. 1. The gate function $g(x)$ is shown in the first panel (*dashed-dotted line*).

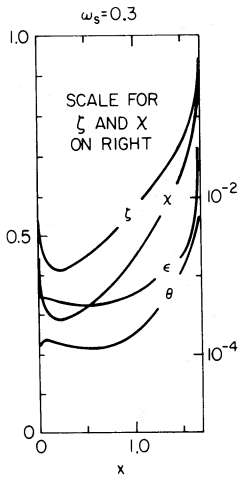

FIG. 3.—Vertical structure of the boundary layer for a star of fastness $\omega_s = 0.3$ and the canonical values of the boundary-layer constants (see Fig. 2). Shown are the vertical semithickness ϵ, temperature θ, density ζ, and pressure χ, in appropriate dimensionless units (see text). Note that the variables ζ and χ are plotted on a logarithmic scale.

case, since the screening currents are concentrated near the disk plane. An accurate calculation of this factor requires quantitative knowledge of the magnetospheric field all the way from the stellar surface to r_0, however, and therefore must await a detailed mathematical description of the accretion flow between r_0 and r_f.

Consider now the variables that describe the vertical structure of the boundary layer. Their variation through the boundary layer is shown in Figure 3 for the case $\omega_s = 0.3$ (rotators with other values of ω_s have very similar vertical structures). The density at the outer edge is comparable to the density of a standard disk. It first decreases inward as the radial velocity increases and matter is lost from the disk, then passes through a minimum, and finally increases inward as the radial velocity decreases. The behavior of the boundary-layer temperature follows from that of the density. Since the heat dissipated in the layer is transported vertically by radiation, the radiant-energy density, which varies as T^4, is directly proportional to the rate of energy generation per unit volume by magnetic field dissipation, which scales as the energy density $B_z^2/8\pi$ of the magnetic field, and inversely proportional to the mean free path of the photons, which scales as ρ^{-1} (since electron scattering is the dominant source of opacity). At the outer edge of the layer, T is comparable to the standard disk temperature. Going inward, T first decreases as $B_z^2/8\pi$ rises only slowly and ρ quickly falls. Subsequently, T becomes roughly constant as the increase in $B_z^2/8\pi$ roughly balances the decrease in ρ. This constant temperature is $\sim$0.1–0.3 of the standard disk temperature, since in this region ρ is $\sim 10^{-2}$–10^{-3} times the standard disk density while the energy dissipation rate is $\sim$0.1–1 times that in a standard disk.

IV. THE OUTER TRANSITION ZONE

We turn now to a detailed calculation of the structure of the outer transition zone. We first present the equations that describe the flow in this zone and compare them with the corresponding equations of the standard disk model. We then introduce the boundary conditions and show that the equations can be solved in a manner similar to that of the α-disk. Finally, we discuss the character of the solutions, paying special attention to the behavior of the residual magnetospheric field.

a) Equations

Equations to describe the accretion flow and the magnetic field configuration in the outer transition zone can be obtained by generalizing the set of standard disk equations so as to include the effects of the residual magnetospheric field which threads the disk in this zone. This generalization consists of both modifying some of the standard disk equations and adding some new equations.

First, however, two equations can be taken over unchanged from the standard disk model. These are the equation of state (15) and the equation of hydrostatic equilibrium in the vertical direction, that is, equation (13) with C_p set equal to unity.

Three further equations can be obtained by modifying standard disk equations. The first of these is the equation which expresses angular-momentum conservation,

$$(d/dr)[\dot{M}r^2\Omega_K + 4\pi\eta hr^3(d\Omega_K/dr)] = B_\phi B_z r^2 . \quad (35)$$

Here η is the coefficient of effective viscosity. The new term on the right-hand side takes into account the angular momentum transported by the magnetic stress associated with the twisted stellar field lines. The second equation obtained by modifying a standard disk equation is the one which describes the vertical radiative transport of the energy dissipated in the disk,

$$\tfrac{1}{3}caT^4/\rho h\bar{\kappa} = \eta hr^2(d\Omega_K/dr)^2 + (J^2/\sigma_{\rm eff})h . \quad (36)$$

Here $\bar{\kappa}$ is the Rosseland mean opacity. The two terms on the right-hand side represent the two dissipative processes by which energy is generated in this zone. The first is the usual one representing viscous dissipation, while the second describes the resistive dissipation of the current generated by the cross-field motion of the plasma.

The third modified equation is the one which defines the α-model of the dissipative stresses. The expression on the right-hand side of equation (36) can be regarded as representing the energy dissipated through an effective stress $W_{\rm eff}$ at the Keplerian rate of strain $(rd\Omega_K/dr)$, and can therefore be written as $W_{\rm eff}(rd\Omega_K/dr)h$. The stress $W_{\rm eff}$ then consists of two parts, the usual effective viscous stress, $\eta(rd\Omega_K/dr)$, and the magnetic stress associated with the residual magnetospheric field. The following arguments show that $W_{\rm eff}$ cannot exceed the thermal pressure p. The effective "viscous" stress, due to turbulence or

the reconnection of small-scale magnetic fields in the plasma, cannot exceed p, since neither the turbulence nor the small-scale magnetic field can attain superthermal energy density (Shakura and Sunyaev 1973). Similarly, the magnetic stress associated with the residual stellar magnetic field threading the disk plasma cannot exceed p, since such a strong stellar field would disrupt the disk. Thus we can write $W_{\rm eff}$ in the form $W_{\rm eff} = \alpha p$, where the parameter α is less than or of order unity; we *assume* that α is constant on a length scale $\sim r$. This equation and equation (36) are then completely analogous to the corresponding equations in the standard disk model of Shakura and Sunyaev (1973), and can be used to solve for the vertical structure of the outer transition zone in the usual way.

Finally, we need to determine the magnetic field configuration in this zone. As mentioned in § II*b*, shear in the toroidal velocity field generates a toroidal magnetic field from the existing poloidal field, and this is further amplified by the converging flow. At the same time, the growth of the toroidal field is limited by reconnection. As a first approximation, we model this complex process by assuming an amplification rate $\gamma_a|\Omega_{\rm K} - \Omega_s|$, where γ_a is a numerical factor ~ 1, and a reconnection rate $\xi v_{\rm A}/2h$, where $v_{\rm A} = (B_\phi^2/4\pi\rho)^{1/2}$. Then, balancing the growth and decay of B_ϕ gives an average azimuthal pitch

$$\gamma_\phi = \left(\frac{\gamma_a}{\xi}\right) 2h(4\pi\rho)^{1/2} \left| \frac{\Omega_{\rm K} - \Omega_s}{B_z} \right| . \qquad (37)$$

Assuming the flow to be steady, this pitch determines the effective conductivity of the disk plasma for poloidal currents, via equation (11). We further assume that the effective conductivity of the disk plasma for toroidal currents is the same as for poloidal currents, and that the ratio γ_a/ξ is constant throughout the outer transition zone. Adding equations (8) and (9) then completes the description of the magnetic field.

b) Boundary Conditions and Method of Solution

As in the standard model, the angular velocity in the outer transition zone is assumed to be Keplerian. The ratio γ_a/ξ is fixed by requiring that γ_ϕ join smoothly to its value γ_0 at r_0. Given a trial vertical disk structure, this boundary condition, together with equations (9) and (11), determines the screening current J, the residual poloidal magnetic field B_z, and the energy-dissipation rate due to cross-field motion. The last determines the new vertical structure, which can be compared with the trial structure, and the procedure can then be iterated until a self-consistent vertical disk structure and residual magnetic field is found.

c) Character of the Solutions

The structure of the outer transition zone is very similar to that of a standard disk at the same radius, as may be seen from Figure 4, which compares the temperature, density, and vertical thickness in this region to the corresponding quantities in a standard disk.

Consider now the magnetic field configuration in this zone. The poloidal field is screened on a length scale $\sim r$ by the azimuthal current $J_\phi = -\sigma_{\rm eff} c^{-1} v_r B_z$ generated by the radial cross-field drift of the plasma. We can express this screening by writing $B_z = \mu b_0 r^{-3} - B_s$, indicating that the stellar dipole field, screened to a fraction b_0 of its unscreened value by the boundary-layer currents, is further reduced by the screening field B_s. Solving for B_s using standard techniques, one finds

$$B_s = \gamma_0 \epsilon_0^{-2} \alpha (h_s/r_0)^2 (1 - \omega_s)^{-1} \epsilon^{-1} f(y) y^{-47/40} B_z(r_0), \qquad (38)$$

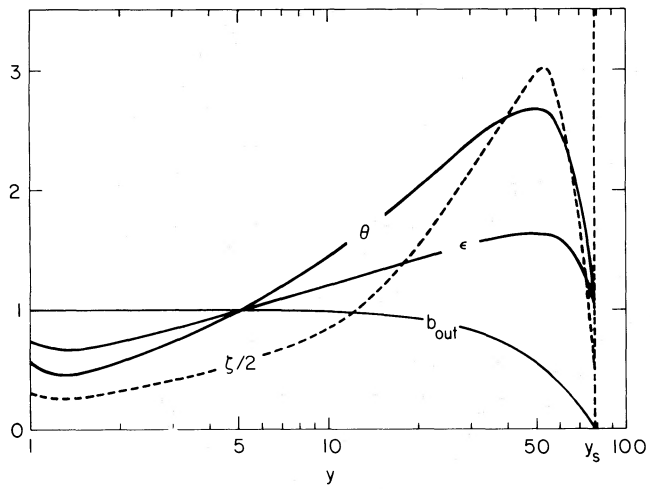

FIG. 4.—Structure of the outer transition zone for a star of fastness $\omega_s = 0.3$. Shown are the vertical semithickness ϵ, temperature θ, and density ζ, in appropriate dimensionless units (see text) as a function of the dimensionless radius $y \equiv r/r_0$. Also shown is the residual poloidal magnetic field, $b_{\rm out} = B_z/\mu b_0 r^{-3}$. The point $y = y_s$ marks the outer edge of the transition zone.

where $\epsilon_0 = \epsilon(r_0)$,

$$f(y) = \frac{1}{2}\left[\left(\frac{2}{n} - 1\right)\int_0^1 F(t^{2/n})dt + \left(\frac{2-n}{3-n}\right)\int_{t^{n-3}}^1 F(t^{2/(3-n)})dt + y^{n-3}F(y^{-2})\right], \quad n = 40/47, \quad (39)$$

in terms of the hypergeometric function $F(t) = {}_2F_1(3/2, 1/2, 2, t)$, and $y = r/r_0$ is the dimensionless radius. The function f, which is ~ 3 at $y = 1$, decreases monotonically with increasing y, closely approaching its asymptotic value 0.78 for $y \gtrsim 3$. The z-component of the magnetic field in the outer transition zone is conveniently described by the dimensionless variable

$$b_{\rm out} \equiv B_z/\mu b_0 r^{-3} = 1 - [f(y)/0.78](y/y_s)^{73/40}. \quad (40)$$

The form of the right-hand expression emphasizes the fact that $f(y)$ reaches its asymptotic value at $y = y_s$ (see below).

Two approximations have been made in obtaining the solution (40). First, in writing B_z in the form $\mu b_0 r^{-3} - B_s$ it has been assumed that the screening currents *inside* r_0, consisting of (*i*) the boundary-layer currents and (*ii*) the currents generated by the cross-field flow between the boundary layer and the flow-alignment radius r_f, reduce the basic dipolar field of the star to *exactly* that of a dipole of moment μb_0. This does not follow from the boundary-layer solutions presented above. However, the facts that (1) $B_z(r_0) = \mu b_0 r_0^{-3}$, and (2) the *total* screening currents inside r_0 reduce the stellar field at radii $\gg r_0$ to roughly that of a dipole of moment μb_0, mean that the dipolar approximation is good except for higher multipole components in B_z which may be significant at radii less than or of the order of several times r_0. The calculation of these higher multipoles is another refinement which must await a quantitative description of the accretion flow and the magnetic field configuration in the region between the boundary layer and the flow-alignment radius r_f.

The second approximation made in obtaining the solution (40) was to assume that $\sigma_{\rm eff}$ is given by equation (11) with γ_ϕ given by equation (37). Among other things, this implies $\sigma_{\rm eff} \propto |B_z|^{-1}$, which leads to a very large value of $\sigma_{\rm eff}$ at large radii. In reality, $\sigma_{\rm eff}$ is limited by dissipative processes other than reconnection which are not included in equation (37). Thus a better approximation is to use the result (40) inside the screening radius

$$y_s \equiv r_s/r_0 \approx 103\alpha^{-32/73}\gamma_0^{-40/73}(1 - \omega_s)^{56/73}, \quad (41)$$

where B_z first vanishes, and $B_z \equiv 0$ outside. This approximation is shown in Figure 3.

The azimuthal pitch γ_ϕ of the magnetic field can be calculated from equation (37) and the known vertical structure of this zone. The result is that as r increases from r_0, γ_ϕ increases from γ_0, passes through a maximum value $\sim\gamma_0$, then decreases, changes sign at the corotation point $r_c = (GM/\Omega_s^2)^{1/3}$, where $\Omega_{\rm K} = \Omega_s$, and remains negative for $r > r_c$. $|\gamma_\phi|$ increases with increasing radius for $r > r_c$, scaling roughly as $r^3 b_{\rm out}^{-1}$ for $r \gg r_c$. Thus the magnetic field lines between r_c and r_s are swept backward and therefore exert a spin-down torque on the star. Most of the spin-down torque comes from the region where $\gamma_0 \lesssim |\gamma_\phi| \lesssim 10^5\gamma_0$, as we show in a subsequent paper (Ghosh and Lamb 1979).

V. DISCUSSION

In the previous sections we have outlined a model for disk accretion by magnetic neutron stars and have used it to construct detailed solutions describing the radial and vertical structure of the accretion flow in the transition zone between the corotating magnetosphere and the disk. In the present section we discuss these solutions, describe some of the implications for neutron-star X-ray sources, and briefly compare our results with other work.

a) General Character of the Present Solutions

The structure of the transition zone found in §§ III and IV, namely, a narrow inner boundary layer where most of the screening occurs, together with a broad outer zone where the residual stellar flux threads the disk, appears to be a general feature of steady, axisymmetric disk accretion, as we now discuss.

In the accretion disk, $\Omega \approx \Omega_{\rm K}$, the force of gravity and centrifugal force closely balance, and the radial-flow velocity is determined by the effective viscous shear stress, which is relatively weak and scales roughly as $r^{-5/2}$. The disk ends where the azimuthal velocity begins to depart significantly from the Keplerian value. This occurs where the torque exerted on the disk plasma by the stress of the stellar magnetic field, which tries to enforce corotation, is large enough to brake the azimuthal motion in a radial distance $\delta \ll r$. Thus the inner radius r_0 of the disk is determined implicitly by the relation

$$(rB_zB_\phi/4\pi)_0 2\pi r_0 2\delta \approx (r\rho v_r \Delta v_\phi)_0 2\pi r_0 2h, \quad \delta \ll r, \quad (42)$$

which also follows from equation (6). That there must be such a point may be seen as follows. Where the stellar magnetic field begins to control the azimuthal motion, one expects $B_\phi \sim B_z$, so that in the absence of screening the left side of equation (42) scales roughly as $(\delta/r)r^{-3}$, whereas for disk flow the right side scales roughly as $r^{1/2}$. Screening steepens the radial dependence of the magnetic field and only strengthens this conclusion. Viscous stresses do not appear in equation (42) because they are too weak, in a thin disk, to disrupt the Keplerian motion; thus, at the point where the magnetic stress becomes large enough to disrupt

this motion, the viscous stress is, of necessity, negligible (the viscous stress is negligible even within the boundary layer, as shown below).

Consider now the width δ of the angular-velocity transition zone or boundary layer. Even if there were no screening, this width would be only a fraction of the radius where it occurs, because of the steep radial dependence of B^2. But the radial motion of the disk plasma is perpendicular to the poloidal magnetic field of the star, creating an azimuthal electric field which drives toroidal currents. These currents screen the poloidal magnetic field, confining it and reducing the width of the transition zone to the electromagnetic screening length,

$$\delta = \frac{c^2}{4\pi\sigma_{\rm eff} v_r} \,. \tag{43}$$

Here $\sigma_{\rm eff}$ is the effective conductivity for toroidal currents. Now the effective conductivity of the disk plasma for *poloidal* currents is related to the toroidal component of the magnetic field; in the boundary layer, where $B_\phi \approx B_z$ and the flow is steady, this conductivity satisfies equation (11) with $\gamma_\phi \sim 1$. To the extent that the same conductivity can be used to evaluate equation (43), one obtains the result

$$\delta \sim (1 - \omega_s)(v_{\rm K}/v_r)h \,, \tag{44}$$

where $\omega_s \equiv \Omega_s/\Omega_{\rm K}$ and $v_{\rm K} = (GM/r_0)^{1/2}$. This is sufficient to show that the angular-velocity transition zone is narrow ($\delta \ll r_0$), as follows.

First, suppose δ were instead $\sim r_0$. From equation (44), this would require $v_r \sim (h/r_0)(1 - \omega_s)v_{\rm K}$. Since the typical value of Ω in the boundary layer, although greater than Ω_s, is less than $\Omega_{\rm K}$, the gravitational force is not completely balanced by the centrifugal force there, and will lead to a typical inward velocity of magnitude

$$v_r \sim (\delta/r_0)^{1/2}(1 - \omega_s^2)^{1/2} v_{\rm K} \,, \tag{45}$$

which for $\delta \sim r_0$ is much larger than allowed by equation (44). A self-consistent solution might still be possible if the radial component of the magnetic pressure gradient, $\partial B^2/\partial r$, were large enough to balance the net radial force $\sim(1 - \omega_s^2)\rho g$. But from equation (42), $\partial B^2/\partial r \approx (h/r_0)^2(1 - \omega_s)^2\rho g$, which is too small. Thus $\delta \sim r_0$ is not self-consistent.

Ignoring for the moment the radial component of the magnetic pressure gradient, equations (44) and (45) can be solved for the self-consistent width of the boundary layer, with the result,

$$\delta/r_0 \sim (1 - \omega_s)^{1/3}(1 + \omega_s)^{-1/3}(h/r_0)^{2/3} \ll 1 \,. \tag{46}$$

That the magnetic pressure gradient does provide some support in the self-consistent solution may be seen by substituting the result (46) into equation (42) and is also evident in Figures 1 and 2, which show that v_r decreases near the inner edge of the boundary layer where this gradient is greatest. The value of the ratio γ_a/ξ that emerges from the numerical solutions is in the range 0.1–3 for $\gamma_0 = 1$, which is consistent with reconnection being the dominant magnetic field dissipation process in and near the boundary layer.

Next, consider the overall effect of the azimuthal screening currents flowing in the boundary layer on the magnetic field configuration. These screening currents cannot completely shield the disk outside r_0 from the stellar magnetic field, since the magnetic field that they produce falls off more steeply with radius than r^{-3}. Thus, even if these currents were to screen the disk at r_0, they would fail to screen the disk outside the boundary layer, and some of the magnetic flux from the star would therefore penetrate this part of the disk as a result of the threading processes described in § II*a*. However, the numerical calculations of § III indicate that the azimuthal currents in the angular-velocity transition zone screen off only $\sim 80\%$ of the stellar magnetic field even at r_0. This screening factor appears to be quite insensitive to the structure of the boundary layer. Hence the full transition zone extends outward some distance beyond the angular-velocity transition zone at r_0.

Finally, consider the extent of this outer part of the transition zone, where the angular velocity is Keplerian but there is still an appreciable magnetic coupling between the star and the disk. The slow radial drift of the disk plasma in this region generates toroidal screening currents in the same way as in the inner transition zone, but the currents here are much weaker due to the smallness of v_r. The quantitative calculations of § IV, which assume a stationary flow and an isotropic conductivity tensor, indicate that the zone of appreciable coupling typically extends outward to several times r_0. The present solutions for the magnetic field configuration are unreliable at larger radii, where they depend sensitively on the model of magnetic field dissipation adopted and predict values of γ_ϕ which are quite large. Nevertheless, the nature of the outer transition zone and the qualitative behavior of the accretion torque will be unaffected by improvements in the treatment of this region so long as the screening length remains $\gtrsim r$, a result which seems relatively secure.

In summary, the two-part structure of the transition zone in the present solutions seems likely to be a general feature of steady, axisymmetric disk accretion. Furthermore, the arguments presented here show that the inner radius of the disk and the width of the boundary layer do not depend on the details of the magnetic field dissipation process but only on the existence of a steady flow, the isotropy of the conductivity, and the reasonable assumption that $\gamma_\phi \approx 1$, where the magnetic field begins to control the flow.

b) Existence of a Maximum Fastness

In our model, stationary inflow solutions can be found only for values of the fastness parameter ω_s less than a certain maximum fastness $\omega_{\rm max} \approx 1$. The reason for this is that when $\omega_s > \omega_{\rm max}$ the centrifugal force on the plasma in the boundary layer is so great that the net radial force at r_0, which has gravitational,

centrifugal, and magnetic components, is outward and so large that the inflow velocity falls to zero in a distance much less than δ_0. We speculate that unsteady accretion may occur for values of ω_s larger than but comparable to ω_{max}, while for $\omega_s \gg \omega_{max}$, disk accretion may cease altogether (compare Davidson and Ostriker 1973; Lamb, Pethick, and Pines 1973).

The range of values of μ, M, $\dot{M}$, and spin period P which satisfy $\omega_s < 1$ can be estimated from equation (24). Given μ, M, and $\dot{M}$, steady-flow solutions can be found only if P exceeds a certain critical value P_{min}. Conversely, given μ, M, and P, such solutions can be found only if $\dot{M}$ exceeds a certain critical value $\dot{M}_{min}$.

c) *Nature of the Boundary Layer*

The boundary layer has several novel and interesting features:

1. It is an electromagnetic boundary layer, in that the dominant stresses are magnetic, rather than viscous as in ordinary shear boundary layers. This follows from equations (13), (42), and (45), which show that the ratio of the magnetic stress $\sim B_z B_\phi/4\pi$ to the viscous stress $\sim \eta r \partial\Omega/\partial r$ is $\gtrsim (r_0/h)^{2/3}(1+\omega_s)^{1/3}(1-\omega_s)^{-1/3}$. Thus the neglect of the viscous stress in the boundary layer (§ III) is valid.

2. The radial inflow is supersonic throughout most of the layer. This follows from equations (13) and (45), which imply $v_r/c_s \approx (r/h)^{2/3}(1-\omega_s^2)^{1/2} \sim 20$. Were the structure of the boundary layer determined by the viscosity instead of the magnetic field, the radial velocity could not exceed the sound speed, since the effective viscous stress cannot exceed the thermal pressure.

3. Energy generation within the boundary layer is the result of resistive dissipation of electrical currents flowing there, rather than viscous dissipation, and occurs at a rate $\sim GM\dot{M}/r_0$. This rate is comparable to the rate of energy generation throughout the outer transition zone. The temperature in the boundary layer is also comparable to that in the outer transition zone near r_0, and is $\sim$0.1–1 times the temperature ($\sim$100 eV) of a standard disk at r_0 (see Fig. 3). Thus, the UV and soft X-ray emission from the boundary layer is not readily distinguishable from that emitted by the broad outer transition zone.

d) *Flow from the Boundary Layer to the Neutron Star*

In constructing the present flow solutions we have assumed that the flow from the boundary layer to the neutron star is channeled by the poloidal magnetic field. A thorough discussion of this assumption would require a detailed knowledge of the magnetic field and the flow in this region. Here we simply outline the nature of the problem.

The accretion flow in the magnetosphere between the disk plane and the star divides naturally into two parts: (1) the flow between the disk plane and the flow-alignment radius r_f and (2) the flow between r_f and the surface of the star. We consider these two regions in reverse order.

The flow between r_f and the stellar surface is, by definition, completely field-aligned in the corotating frame of the star (see Paper I). Lamb and Pethick (1974) first pointed out that within the magnetosphere such a flow is stable only if it is sub-Alfvénic, and that this condition therefore limits the extent of the stable magnetosphere; detailed calculations performed since then (Williams 1975; Adam 1978) have clarified the nature of the instability that occurs in a field-aligned flow which passes from super-Alfvénic to sub-Alfvénic. A necessary condition for the stability of the accretion flow interior to r_f is therefore that the Alfvénic Mach number, $\mathcal{M}_A \equiv v_\parallel/v_A$, not cross unity from above anywhere in this region. Here $v_\parallel$ is the flow velocity along the magnetic field and v_A is the Alfvén velocity in the poloidal magnetic field. A determination of the field strength, plasma density, and velocity over the accretion bundle requires a detailed knowledge of the accretion flow at the flow-alignment surface. However, even without such knowledge one can estimate the Alfvén Mach number averaged over the accretion bundle, assuming that the magnetic field is dipolar in this region. Then the cross-sectional area of the accretion bundle is

$$a(r) \approx 4\pi r^2(\delta/r_0)(r/r_0)[4 - 3(r/r_0)]^{-1/2} . \quad (47)$$

Using equations (29), (30), and (47), the equation of continuity, and the values of the boundary-layer constants chosen in § III, one finds

$$\langle \mathcal{M}_A \rangle \approx (v_\parallel/v_{ff})^{1/2}(r/r_0)^{5/4}[4 - 3(r/r_0)]^{-1/4}(B_0/B_p) , \quad (48)$$

where $B_0 = \mu r^{-3}[4 - 3(r/r_0)]^{1/2}$ is the typical strength of the unscreened poloidal field along the accretion bundle. Clearly, $\langle \mathcal{M}_A \rangle$ is less than unity for $r \leq r_f < r_0$ since $v_\parallel \leq v_{ff}$ and $B_p > B_0$. Given $\langle \mathcal{M}_A \rangle < 1$, we expect that $\mathcal{M}_A < 1$ over most of the cross section of the flow, and hence that the flow inside the flow-alignment surface is stable.

The corresponding stability condition for the flow between the disk plane and r_f is not known, since the stability of magnetohydrodynamic flows in the presence of finite electrical conductivity and appreciable cross-field motion has not been studied in detail. It seems likely, however, that a sufficient condition for the flow in this region to be stable is $\mathcal{M}_A < 1$. The Alfvén Mach number of the vertical flow at the disk plane can be calculated over the entire accretion bundle using the boundary-layer solutions obtained in § III. In terms of the dimensionless boundary layer variables, the result is

$$\mathcal{M}_A \simeq \left(\frac{h_s}{r_0}\right)^{1/2}\left(\frac{\delta}{r_0}\right)^{1/4}\left[\left(\frac{g\epsilon F}{bu_r}\right)^{1/2}\right] \quad (49)$$

and is shown in Figure 5 for the case $\omega_s = 0.3$. At this point the flow is sub-Alfvénic over the entire accretion bundle. The average Mach number well above and below the disk is given by equation (48), to the extent that the cross-sectional area of the

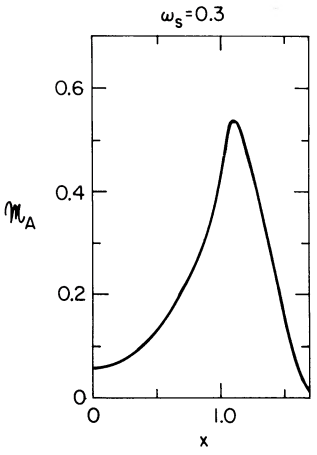

FIG. 5.—Alfvén Mach number $\mathcal{M}_A$ of the flow in the accretion bundle just above and below the disk plane as a function of the boundary-layer coordinate x, for a star of fastness $\omega_s = 0.3$.

accretion bundle in this region is given by equation (47) and no mass is lost from the accretion bundle due, for example, to Rayleigh-Taylor instability (the latter would lower the Mach number). The quantities that appear in equation (48) take the values $(v_\parallel/v_{ff})^{1/2} \sim 0.1$, $(r/r_0)^{5/4}[4 - 3(r/r_0)]^{-1/4} = 1$, and $0.5 \lesssim (B_0/B_p) \lesssim 5$, at the disk plane. With increasing distance away from the plane, $v_\parallel/v_{ff}$ increases slowly, while $(r/r_0)^{5/4} \times [4 - 3(r/r_0)]^{-1/4}$ rapidly decreases, and B_0/B_p approaches unity. It therefore seems likely, though not certain, that $\mathcal{M}_A < 1$ also holds between the disk plane and the flow-alignment surface.

e) *Implications for X-ray Emission from the Stellar Surface*

The topology of the accretion bundle found here, with appreciable flux threading the disk outside the boundary layer, implies that matter within the bundle collides with the stellar surface in polar rings of radius $R_r \sim 0.3(R/r_0)^{1/2}R$ and width $\delta_r \sim 0.5(R/r_0)^{3/2}\delta \sim 0.12R_r$, where R is the stellar radius. The area of each ring is typically $\sim 10^9$ cm^2, giving a lower limit to the temperature of the emitting region of $9 \times 10^7(M/M_\odot)^{1/28}\mu_{30}^{1/7}L_{37}^{5/28}R_6^{-23/28}$ K, assuming that all the accreting matter is channeled within the accretion bundle by the stellar magnetic field.

In reality, all matter need not be channeled to the magnetic poles of the star. In its flow out of the disk plane toward the star, the accreting matter is supported against the gravitational force of the star by the pressure of the stellar magnetic field. This situation is Rayleigh-Taylor unstable, and, depending on the relation between the growth time of the instability and the time of infall from r_0 to the stellar surface, may allow significant amounts of matter to penetrate near the stellar surface without becoming flux-frozen (Elsner and Lamb 1976, 1977; Arons and Lea 1976). The motion of matter entering the magnetosphere in this way and its implications for pulse shapes and spectra of pulsating X-ray sources has been discussed by Elsner and Lamb (1976). The accretion bundles near the disk plane are particularly likely to be unstable, since the centrifugal support due to motion along the curved field lines of the bundle is small there.

f) *Implications for Period Changes in Pulsating X-ray Sources*

In Paper I we derived bounds on the accretion torque by applying conservation laws and discussed the implications for spin-up and spin-down of the neutron star. In particular, we showed that if the star were accreting from a disk rotating in the same sense as the star and if the transition zone were narrow (width $\ll r_0$), then the accretion torque N would satisfy the inequality

$$\tfrac{1}{2}(1 + \omega_s)N_0 \leq N \leq N_0\,, \tag{50}$$

where $N_0 = \dot{M}(GMr_0)^{1/2}$ and ω_s is the fastness parameter, which satisfies $0 \leq \omega_s \lesssim 1$. Thus, if the transition zone in disk accretion were narrow, fast as well as slow rotators would experience a spin-up torque $\approx N_0$. This in turn would make it difficult to understand the behavior of a fast rotator like Her X-1 which is surely accreting from a disk but shows a spin-up rate ~ 40 times smaller than would be implied by an accretion torque $\sim N_0$ (Elsner and Lamb 1976). Even an arbitrarily small stellar magnetic field would not be sufficient to reconcile this discrepancy, contrary to the conclusion of Scharlemann (1978), who postulated a narrow transition zone but a minimum accretion torque very much smaller than that allowed by inequality (50) (such a small accretion torque would require a substantial violation of energy conservation).

The present calculations show that there is, in fact, no conflict between the theoretical and observed spin-up rates, since the transition zone in disk accretion generally is *not* narrow. In a subsequent paper (Ghosh and Lamb 1979), we use the accretion-flow solutions constructed here to show that the magnetic coupling between the disk and the star due to the stellar field lines which thread the disk in the broad transition zone is appreciable, and can be the dominant component of the accretion torque when the stellar angular velocity is sufficiently large. As a result, the accretion torque on fast rotators is generally less than N_0 and can even become negative (braking the star's rotation) while accretion, and hence X-ray emission, continues. The calculated secular spin-up rates are in quantitative agreement with the observed values for magnetic moments $\mu \sim 10^{29}$–10^{32} gauss cm^3.

g) *Comparison with Oblique Rotators*

We have investigated here the problem of axisymmetric accretion by aligned rotators because of its mathematical simplicity. On the other hand, the *pulsating* X-ray sources, at least, are almost certainly oblique rotators. Accretion by such stars will have several new features, four of which we note here.

First, because the magnetospheric boundary in the

disk plane will no longer be circular, the magnetic forces acting on the disk plasma will be time dependent in the inertial frame and magnetic pressure gradients will affect the azimuthal, as well as the radial, motion. Although some of the details of the coupling between the star and the accreting plasma are certain to be altered, we expect the basic features of the flow that have emerged from the present calculations to be present, including the narrow shear boundary layer and the more extended region of magnetic coupling, and the inner radius of the disk to be determined by a condition analogous to equation (42).

Second, only a subset of the magnetic field lines threading the boundary layer are likely to contain large amounts of accreting plasma. This is because field lines threading the boundary layer at other azimuths will be so tilted that the maximum of the gravitational potential along with them will occur far from the disk plane; matter accreting along field lines will therefore reach the stellar surface over only an arc of the "hot ring" described above, in a manner similar to that assumed by Basko and Sunyaev (1976).

Third, the cross section of the accretion column will not be a *circular* arc since (as noted above) the distortion of the magnetospheric field by electrical currents flowing in the disk will no longer be axisymmetric.

Fourth, the accretion torque acting on the star will have a component perpendicular as well as parallel to the rotation axis. Such a torque component could play an important role in pumping or damping free precession of the star (see Lamb *et al.* 1975).

h) Comparison with Other Work

It may be helpful to compare the results of the present calculations with other work. We first compare the physical criterion that determines the inner radius of the disk in the hydromagnetic solutions found here with criteria suggested previously in the literature. Previous suggestions can be divided into three types according to whether they assume that the inner radius is determined by energy, stress, or pressure balance. After briefly discussing each of the three types of criteria and the values of r_0 that they predict, we conclude by comparing the plasma flows assumed in some recent treatments of disk accretion with those expected on the basis of the present solutions.

Lamb, Pethick, and Pines (1973) identified the inner radius of the disk with the radius at which the stellar magnetic field begins to channel the accretion flow. They assumed that the magnetic field rapidly threads the accreting plasma and therefore begins to channel the flow at the Alfvén radius r_A, where the flow becomes sub-Alfvénic in the stellar magnetic field (see Paper I). In the absence of a detailed model of the flow, they estimated r_A by calculating the radius where the energy density of the dipole magnetic field equals that of the accreting plasma as seen in the corotating frame or, in other words, where $B^2/8\pi \approx \frac{1}{2}\rho v^2$; here v is the velocity of the plasma in the corotating frame (cf. Paper I, eq. [19]). In evaluating this expression, Lamb *et al.* adopted $v \sim r\Omega_K$ and a density comparable to that in the disk plane, with the result $r_0 \sim (h/r)^{2/7} \times (v_r/v_{ff})^{2/7} r_A^{(0)}$, where v_r is the radial velocity of the plasma just outside the Alfvén surface. If v_r in this expression is evaluated using the typical radial velocity $(\delta/r_0)^{1/2} v_{ff}$ in the boundary layer and the result (29) for δ, one obtains the estimate $r_0 \sim 0.20 C_\omega^{1/7} r_A^{(0)}$, while if v_r is evaluated using the radial velocity in the disk outside the boundary layer, the resulting estimate of r_0 is still smaller. On comparing these results with equation (30), we conclude that this expression somewhat underestimates r_0 in the case of axisymmetric disk accretion by an aligned rotator.

Lamb and Pethick (1974) argued, for reasons similar to those given above in § V*a*, that the stellar magnetic field first dominates the accretion flow where the magnetic stresses are comparable to the material stresses; this criterion is equivalent to equation (42) if $\delta \sim h$ (the algebraic expression given by these authors, namely $\rho v_r v_\phi \sim B_r B_\phi / 4\pi$, is more appropriate to an oblique rotator, but gives the same value of r_0 as eq. [42] if $B_r \sim B_z$ at r_0 and $\delta \sim h$). Rees (1974) suggested a similar condition, $\rho v_r v_\phi \sim B^2/4\pi$, to determine r_0; this is equivalent to equation (42) if $B_\phi \sim B_z$ at r_0 and $\delta \sim h$. Since the present model assumes $B_\phi \approx B_z$ at r_0 and determines δ to be $\sim 4h$ (the latter follows from eq. [46]), the values of r_0 given by these dimensional estimates roughly agree with the value obtained from the more detailed calculations described here.

Finally, consider the estimates that were based on the idea of pressure balance. Pringle and Rees (1972) suggested that the magnetospheric boundary would be located where the pressure of the stellar magnetic field balances the gas pressure in the disk, that is, where $B^2/8\pi \sim p_{disk}$. This criterion gives the estimate $r_0 \sim 0.57 x^{-2/7} y^{2/7} r_A^{(0)}$, if one uses the disk model of these authors, or $r_0 \sim 0.26 \alpha^{2/7} r_A^{(0)}$, if one uses the disk model of Shakura and Sunyaev (1973). Scharlemann (1978) modified the Pringle-Rees condition by attempting to take into account the enhancement of the stellar magnetic field B by screening currents at the inner edge of the disk. His modified condition, $(B + \Delta B)^2/8\pi \approx p_{disk}$, where ΔB is the screening field, gave $r_0 \sim 0.86 \alpha^{2/7} r_A^{(0)}$. However, the first two of the three boundary conditions used by Scharlemann to choose a solution are actually the same equation approximated in two different ways. Thus, the inner radius of the disk determined using these boundary conditions is not logically consistent. Ichimaru (1978) modified the Pringle-Rees criterion in a different way by attempting to take into account gravitational and centrifugal forces acting on the plasma in the boundary layer. However, Ichimaru's model is defective in important respects, some of which are noted below. A general question which arises with all criteria based on the idea of pressure balance is the relevance of this static criterion to dynamic accretion flows which penetrate the magnetospheric cavity. At the very least, these criteria ignore both inertial forces (see Elsner and Lamb 1977) and the coupling between the stellar magnetic field and the orbital motion of the plasma which results from the Kelvin-Helmholtz instability and other processes (see § II above).

In summary, the criteria previously proposed for estimating r_0 have quite different physical interpretations and show quite different scalings in terms of the physical parameters of the problem from that of the criterion found from the present detailed calculations. Despite these important differences, the earlier criteria typically give estimates for r_0 which are within a factor of ~ 2 of the value found here, a consequence of the steep radial dependence of the stellar magnetic field and the resulting insensitivity of r_0 to the particular criterion used.

The flow of plasma from the disk toward the star has also been considered recently by Scharlemann (1978) and Ichimaru (1978). Scharlemann stressed the likely importance of the Kelvin-Helmholtz instability in mixing the disk plasma and the magnetospheric field and suggested a model of plasma flow from the inner edge of the disk toward the neutron star which is very similar to the model we have adopted in the present work. Ichimaru proposed a model of the flow in which plasma penetrates into a boundary layer by anomalous diffusion, but his treatment suffers from several deficiencies and inconsistencies. Among them we mention first, that his equation (7) implicitly assumes that the angular velocity of the plasma changes discontinuously from the Keplerian value outside the outer surface of the boundary layer to the stellar angular velocity just inside, even though there are no stresses in the model to effect this change. Second, his equation (29) assumes that the inflowing plasma within the magnetosphere rotates rigidly with the angular velocity of the star and that the flux of angular momentum toward the star is always zero. Both assumptions are too restrictive (cf. Paper I, eqs. [10] and [11]). In particular, the former requires that the stellar field lines be infinitely rigid, while the latter implies that the torque on the star is zero and hence that it spins down as it accretes (see Paper I, § IV.) Third, Ichimaru's equation (31) implicitly assumes that the angular velocity of the plasma inside the magnetosphere is the same as that in the disk outside, contrary to the assumption implicit in his equation (7). Since these two angular velocities are in general different, his equation (31) should include an additional term describing the change in the material stress across the magnetospheric boundary (see Lamb 1975, eq. [27]).

VI. CONCLUDING REMARKS

In the present paper we have described a first calculation of the radial and vertical structure of the transition zone at the magnetospheric boundary of an aligned rotating neutron star accreting matter from a Keplerian disk. The calculation indicates (1) that the inner edge of the disk is located where the integrated magnetic stress acting on the disk plasma becomes comparable to the integrated material stress associated with its inward radial drift and orbital motion; (2) that the stellar magnetic field threads the disk near its inner edge via the Kelvin-Helmholtz instability, turbulent diffusion, and reconnection, producing a broad transition zone between the unperturbed disk flow and the corotating magnetosphere; (3) that the transition zone is composed of two qualitatively different regions, a broad outer transition zone where the motion is Keplerian, and a narrow inner transition zone or boundary layer where the departure from Keplerian motion is substantial; (4) that the stellar magnetic field is largely but not entirely screened by currents flowing in the boundary layer; and (5) that for sufficiently fast stellar rotation there are no steady-flow solutions. The inner radius of the disk and the width of the boundary layer do not depend on the details of the magnetic-flux reconnection process in the boundary layer but only on the existence of a steady flow and a crudely isotropic effective conductivity. Although magnetic flux reconnection is likely to produce fluctuations in the flow, at least on sufficiently small spatial and temporal scales, and hence variations in the size and structure of the boundary layer, the present stationary flow model may provide an adequate description of the average flow toward the star.

In a subsequent paper (Ghosh and Lamb 1979), we use the results obtained here to calculate the torque exerted on the neutron star by the accreting plasma. There we show (1) that the magnetic field which threads the disk in the outer transition zone exerts an appreciable torque on the star; (2) that this torque can dominate the torque due to matter in the boundary layer, if the star is rotating fast enough, braking the star's rotation even while accretion, and hence X-ray emission, continues; (3) that all the secular period changes so far measured in pulsating X-ray sources, including Her X-1, are consistent with disk accretion; and (4) that the short-term period fluctuations and spin-down episodes observed in Her X-1, Cen X-3, and 4U 0900−40 may be explained naturally as consequences of relatively small fluctuations in the mass-accretion rate.

Work is currently under way (1) to develop a more sophisticated treatment of magnetic field amplification and dissipation in the transition zone, (2) to obtain solutions to the hydromagnetic equations that describe the flow between the disk plane and the flow-alignment radius, and (3) to use the understanding gained here to solve for the flow in the disk plane without making the boundary-layer approximation, thereby eliminating all undetermined constants and determining the variation of the azimuthal pitch through the boundary layer.

The present results also suggest several other problems that merit study. These include the mathematical description of the accretion flow in oblique rotators, the stability properties of steady axisymmetric flows of the type considered here, and the time-dependence of reconnection in the transition zone. An understanding of the last two problems would shed light on the origins of fluctuations in the luminosity, pulse period, pulse shape, and spectrum of pulsating X-ray sources, and would provide a basis for evaluating the steady-flow assumption made in the present work. Finally, in view of the qualitative difference

between the transition zone in nearly spherical accretion and that in accretion from a Keplerian disk, it would be interesting to study how the transition zone changes from the one form to the other, by investigating accretion flows in which the infalling matter has sufficient angular momentum to cause appreciable flattening of the flow but not enough to form a thin Keplerian disk.

It is a pleasure to thank Professors D. Q. Lamb, F. C. Michel, C. J. Pethick, J. Petterson, D. Pines, E. T. Scharlemann, and V. Vasyliunas for helpful discussions. We also acknowledge useful correspondence with Professor Scharlemann concerning his work. One of us (F. K. L.) thanks Professor G. Garmire and the Department of Physics at Caltech for their warm hospitality.

REFERENCES

Adam, J. A. 1978, *J. Plasma Phys.*, **19**, 77.
Arons, J., and Lea, S. M. 1976, *Ap. J.*, **207**, 914.
Basko, M. M., and Sunyaev, R. A. 1976, *M.N.R.A.S.*, **175**, 395.
Cole, J. D., and Huth, J. H. 1959, *Phys. Fluids*, **2**, 624.
Davidson, K., and Ostriker, J. P. 1973, *Ap. J.*, **179**, 585.
Eardley, D. M., and Lightman, A. P. 1975, *Ap. J.*, **200**, 187.
Elsner, R. F., and Lamb, F. K. 1976, *Nature*, **262**, 356.
———. 1977, *Ap. J.*, **215**, 897.
Forman, W., Jones, C., Cominsky, K., Julien, P., Murray, S., Peters, G., Tananbaum, H., and Giacconi, R. 1978, *Ap. J. Suppl.*, **38**, 357.
Ghosh, P., and Lamb, F. K. 1978, *Ap. J. (Letters)*, **223**, L83.
———. 1979, submitted to *Ap. J.*
Ghosh, P., Lamb, F. K., and Pethick, C. J. 1977, *Ap. J.*, **217**, 578 (Paper I).
Ichimaru, S. 1978, *Ap. J.*, **224**, 198.
Lamb, D. Q., Lamb, F. K., Pines, D., and Shaham, J. 1975, *Ap. J. (Letters)*, **198**, L21.
Lamb, F. K. 1975, in *Proc. Internat. Conference on X-rays in Space*, ed. D. Venkatesan (Calgary), p. 613.
———. 1977, in *Proc. 8th Texas Symposium on Relativistic Astrophysics, Ann. NY Acad. Sci.*, **302**, 482.
Lamb, F. K., and Pethick, C. J. 1974, in *Astrophysics and Gravitation, Proc. 16th Internat. Solvay Congress* (Brussels: L'Université de Bruxelles), p. 135.
Lamb, F. K., Pethick, C. J., and Pines, D. 1973, *Ap. J.*, **184**, 271.
Lamb, F. K., Pines, D., and Shaham, J. 1976, in *X-Ray Binaries, Proc. Goddard Conference*, ed. E. Boldt and Y. Kondo (NASA SP-389), p. 141.
Lamb, F. K., Pines, D., and Shaham, J. 1978*a*, *Ap. J.*, **224**, 969.
———. 1978*b*, *Ap. J.*, **225**, 582.
Liang, E. P. T. 1977, *Ap. J.*, **218**, 243.
Lightman, A. P., Rees, M. J., and Shapiro, S. L. 1978, in *Proc. Enrico Fermi Summer School on Physics and Astrophysics of Neutron Stars and Black Holes*, in press.
Mason, K. O. 1977, *M.N.R.A.S.*, **178**, 81P.
Mestel, L. 1975, in *Magnetohydrodynamics*, Saas-Fee Lectures 1974, ed. L. Mestel and N. O. Weiss (Swiss Society of Astronomy and Astrophysics).
Michel, F. C. 1977*a*, *Ap. J.*, **213**, 836.
———. 1977*b*, *Ap. J.*, **214**, 261.
———. 1977*c*, *Ap. J.*, **216**, 838.
Midgley, J., and Davis, L. 1962, *J. Geophys. Res.*, **67**, 499.
Northrop, T. G. 1956, *Phys. Rev.*, **103**, 1150.
Parker, E. N. 1971, *Ap. J.*, **163**, 279.
Pounds, K. A. 1977, in *Proc. 8th Texas Symposium on Relativistic Astrophysics, Ann. NY Acad. Sci.*, **302**, 361.
Pringle, J. E., and Rees, M. J. 1972, *Astr. Ap.*, **21**, 1.
Rappaport, S. A., and Joss, P. C. 1977, *Nature*, **266**, 683.
Rees, M. J. 1974, in *Astrophysics and Gravitation, Proceedings of the 16th Internat. Solvay Congress* (Brussels: L'Université de Bruxelles), p. 97.
Scharlemann, E. T. 1978, *Ap. J.*, **219**, 617.
Shakura, N. I., and Sunyaev, R. A. 1973, *Astr. Ap.*, **24**, 337.
Shakura, N. I., Sunyaev, R. A., and Zilitinkevich, S. S. 1978, *Astr. Ap.*, **62**, 179.
Vasyliunas, V. M. 1975, *Rev. Geophys. Space Phys.*, **13**, 303.
Williams, D. J. 1975, *M.N.R.A.S.*, **171**, 537.

P. GHOSH: Code ES62, NASA/MFSC, Marshall Space Flight Center, Huntsville, AL 35812

F. K. LAMB: Department of Physics, University of Illinois at Urbana-Champaign, Urbana, IL 61801